SIMULATION ANALYSIS OF AUTOMATIC CUTTING CONTROL FOR ROADHEADERS

Haoran ZHANG[1], Yonggang LIU[2], Bo CHEN[1,*], Jiyue YANG[1], Yahang WU[1], Lei QIN[3], Longjie LI[4]

In order to achieve the tracking control of the motion trajectory of the cutting head under the vibration interference and improve the cutting efficiency of the roadheader, the kinetic model of the cutting mechanism of the roadheader is established in this paper, and the kinetic equation of the cutting mechanism is established. The reverse kinematics of the cutting mechanism is simulated with MATLAB software, and the motion trajectory equation of the cutting head is determined; Based on the above analysis, the dynamic model of the cutting mechanism is established and the dynamics of the cutting mechanism is analyzed. By introducing the vibration function of the cutting head, the relationship between the vibration function of the cutting head and the external load of the hydraulic cylinder is determined. The motion trajectory tracking control method of the cutting head under vibration interference is proposed. The simulation model of the motion trajectory control system of the cutting head is established by MATLAB/Simulink module. The motion trajectory of the cutting head under vibration interference and the displacement of the piston rod of the hydraulic cylinder are tracked and controlled. The results show that the motion trajectory tracking control method of the cutting head under vibration interference is correct.

Keywords: Cantilever tunnel boring machine, MATLAB, Kinematic simulation, Dynamic analysis, Control of the movement trajectory of the cutting head

1. Introduction

Under the background of safe coal mining and efficient production, tunnel boring machines are developing towards automation and intelligence. The research on the automatic cutting control technology of tunnel boring machines is precisely the key to promoting the rapid development of intelligent tunnel boring machines. Zeki[1] designed symmetrical disc-shaped cutting tools, which reduced the lateral load caused by lateral forces and improved the steering force and

* Corresponding author: 13505386167@126.com
[1] Shandong University of Science and Technology, Taian 271000, China
[2] 248 Geological Brigade of Shandong Nuclear Industry, Qingdao 266600, China
[3] China Academy of Machinery Science & Technology Qingdao Branch Co., Ltd., Qingdao 266300, China
[4] BinZhou Polytechnic, Binzhou 256600, China

balance of the tool disc. Xie[2] monitored the operating status of the tunnel boring machine by integrating multi-sensor information and controlled the automatic cutting operation of the cutting head by constructing an automatic cutting PID control system for the tunnel boring machine, which improved the cutting efficiency. Peng et al. [3] established a virtual prototype of the cutting section of a tunnel boring machine using ADAMS software and a hydraulic system of the cutting section of the tunnel boring machine using Amesim software. On this basis, a joint simulation model of the machine and hydraulic system of the cutting section of the tunnel boring machine was established. By planning the automatic cutting process path of the tunnel section, the precise tracking and control of the movement trajectory of the cutting head was achieved. Zhang[4] et al. solved the problem of obtaining the load of the cutting teeth on the surface of coal and rock by means of discretized digital coal and rock mass construction and chain digital mapping entity construction. They achieved performance simulation of the cutting section and led the experimental calibration with virtual experiments, reducing the cost and safety risks of the experiments. They also optimized the low-stress cutting through the DDPG algorithm. Zhang[5] et al. proposed an improved NSGA-II algorithm. By constructing a kinematic model and a dual-objective optimization function, the computational speed was enhanced and the trajectory deviation of the cut was reduced. Liu[6] aimed at the problem of significant power loss caused by constant-speed coal and rock cutting by roadheaders, designed a variable frequency drive control system for the cutting head, which achieved automatic control of the cutting head's rotational speed and torque, providing guidance for the intelligent cutting of roadheaders. Liang[7] et al. simulated the cutting heads under different working conditions through ABAQUS, established Drucker-Prager as the coal body constitutive model to simulate the coal cutting process, verified the consistency between the simulation and the experiment, and obtained the cutting force laws and torque waveforms under different working conditions through MATLAB It provides technical support for stable control and efficiency improvement of cutting. Ma[8] et al. proposed a cutting head positioning system that combines the cutting head motion model with ultra-wideband positioning technology, verified its anti-interference ability and positioning accuracy, and obtained the main factors affecting the positioning accuracy through field simulation experiments, achieving the accuracy optimization of the positioning system.

In summary, most existing cutting head trajectory control systems ignore load interference and rarely consider the impact of the vibration characteristics of the tunneling machine on the tracking control of cutting head motion trajectory. Therefore, this article will establish a mathematical relationship between the load of the cutting head, the external load force of the hydraulic cylinder, and the vibration function of the cutting head, propose a tracking control method for the

cutting head motion trajectory, and simulate the tracking control of the cutting head motion trajectory and the displacement of the hydraulic cylinder piston rod under vibration interference by constructing a simulation model of the cutting head motion trajectory control system.

2. Reverse kinematics of the cutting mechanism of the roadheader

The kinematic equation of the cutting mechanism establishes the relationship between the pose of the cutting head and the joint variables or the stroke of the hydraulic cylinder. Given the pose of the cutting head, each joint variable and the stroke of the hydraulic cylinder can be calculated through the inverse kinematic equation[9].

The inverse kinematic solution of the cutting mechanism is the basis of trajectory planning and motion control of the cutting head, which is more consistent with the actual application of the project[10]. Through the simulation analysis of the kinematic model of the cutting mechanism, the relationship between the lifting hydraulic cylinder stroke l_1, the rotary hydraulic cylinder stroke l_2 and the horizontal and vertical coordinates (y, z) of the cutting head is determined, so as to determine the position of the cutting head. The simulation parameters of the back solution of the cutting mechanism of the roadheader are shown in Table 1[11, 12].

Table 1

Simulation parameters for inverse kinematics of cutting mechanism

Δl	e	L_x	θ_0	ϕ_0	L_0	L_1
650 mm	700 mm	3747 mm	1.183°	57.13°	1600 mm	571 mm

1) Establish a kinematic model between the spatial position coordinates of the cutting head and the joint variables of the lifting cutting mechanism.

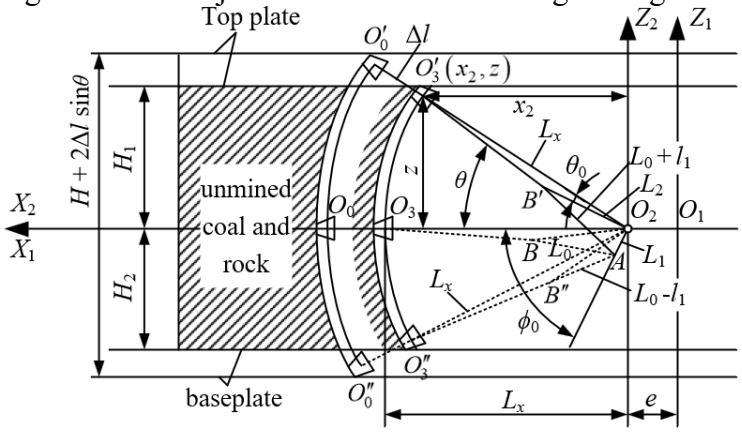

Fig. 1. Vertical swing cutting diagram of cutting mechanism

In Fig. 1, O_1 and O_2 are the horizontal rotation center of the rotary table and the vertical swing center of the cutting arm, respectively. O_3 and O'_3 are the

projections of the cutting head center in the vertical plane when the cutting arm is in the horizontal position and the vertical swing angle is θ; H is the height of the tunnel, A and B are the hinge points between the lifting hydraulic cylinder and the turntable, and between the lifting hydraulic cylinder and the cutting arm, respectively. Set the length of the cutting arm $O_2O_3=L_x$, the initial length of the hydraulic cylinder $AB=L_0$, $O_2A=L_1$, $O_2B=L_2$, $\angle O_3O_2A=\varphi_0$, $\angle O_3O_2B=\theta_0$, and obtain the coordinates (x_2，z) when the cutting head is swinging upward:

$$\begin{cases} x_2 = (L_x+\Delta l)\cos\left\{\cos^{-1}\left(\dfrac{L_1^{\,2}+L_2^{\,2}-(L_0+l_1)^2}{2L_1L_2}\right)-\phi_0+\theta_0\right\} \\ z = (L_x+\Delta l)\sin\left\{\cos^{-1}\left(\dfrac{L_1^{\,2}+L_2^{\,2}-(L_0+l_1)^2}{2L_1L_2}\right)-\phi_0+\theta_0\right\} \end{cases} \tag{1}$$

$$\theta = \cos^{-1}\left(\frac{L_1^{\,2}+L_2^{\,2}-(L_0+l_1)^2}{2L_1L_2}\right)-\phi_0+\theta_0 \tag{2}$$

From equations (1) and (2), it can be seen that l_1 is an unknown variable, and the spatial motion coordinates (x_2, z) of the cutting head only change with the variation of l_1. Therefore, in the actual process of cutting coal and rock by the tunneling machine, the vertical swing of the cutting head can be controlled by controlling the stroke l_1 of the lifting hydraulic cylinder; When the cutting head swings downwards, l_1 needs to be changed to -l_1 and θ needs to be changed to -θ, but the upper and lower limit swing angles of the cutting arm are not equal.

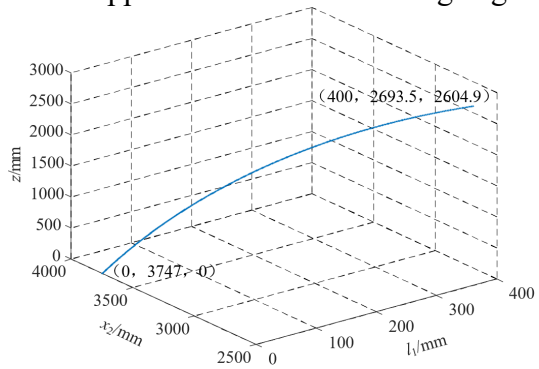

(a) The relationship between the cutting head position and l_1

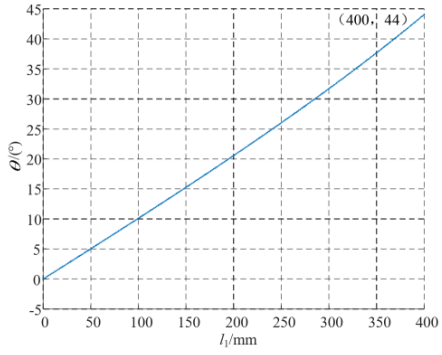

(b) The relationship between the vertical swing Angle θ and l_1

Fig. 2. Vertical oscillation cutting simulation of cutting mechanism

It can be seen from Fig. 2(a), the position coordinate x_2 of the cutting head decreases parabolic from 3747 mm to 2693.5 mm with the increase of l_1, and the coordinate z rises linearly from 0 mm to 2604.9 mm with the increase of l_1. As can be seen from Fig. 2(b), the vertical swing Angle θ increases basically in a straight line with the increase of l_1, and the maximum vertical swing Angle $\theta_{max}=44^\circ$, which is basically consistent with the maximum swing Angle during the actual

cutting process of the tunnel boring machine.

2) Establish a kinematic model between the spatial position coordinates of the cutting head and the joint variables of the rotary cutting mechanism.

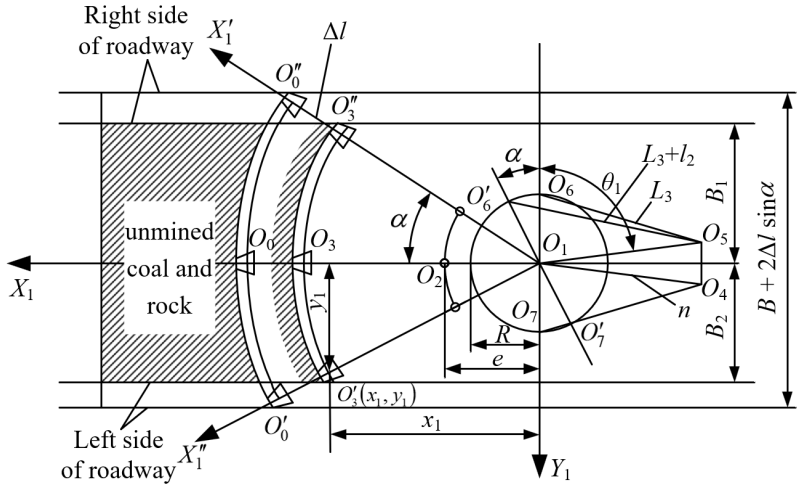

Fig. 3. Schematic diagram of horizontal swing cutting of cutting mechanism

In Fig. 3, α represents the horizontal swing Angle of the rotary cutting mechanism, O'_3 is the projection of the cutting head center in the horizontal plane when the cutting mechanism swings α to the left, B is the width of the roadway, e is the distance from the center of the turntable to the center of the cutting arm, and R is the radius of the rotary table. $\angle O_6O_1O_5=\angle O_7O_1O_4=\theta_1$, $O_1O_4=O_1O_5=n$, $O_4O_7=O_5O_6=L_3$, $O_5O'_6=L_3+l_2$, $O_4O'_7=L_3-l_2$, Obtain the coordinates (x_1, y_1) when the cutting head swings horizontally to the left:

$$\begin{cases} x_1=\left[(e+(L_x+\Delta l)\cos\theta\right]\cos\alpha \\ \quad=\left\{(e+(L_x+\Delta l)\cos\left[\cos^{-1}\left(\dfrac{L_1^{\,2}+L_2^{\,2}-(L_0+l_1)^2}{2L_1L_2}\right)-\phi_0+\theta_0\right]\right\}\cos\alpha \\ y_1=\left[(e+(L_x+\Delta l)\cos\theta\right]\sin\alpha \\ \quad=\left\{(e+(L_x+\Delta l)\cos\left[\cos^{-1}\left(\dfrac{L_1^{\,2}+L_2^{\,2}-(L_0+l_1)^{\,2}}{2L_1L_2}\right)-\phi_0+\theta_0\right]\right\}\sin\alpha \end{cases} \tag{3}$$

$$\alpha=\cos^{-1}\left[\frac{n^2+R^2-(L_3+l_2)^2}{2nR}\right]-\theta_1 \tag{4}$$

From Equations (3) and (4), it can be known that l_1 and l_2 are unknown quantities, and (x_1, y_1) change with the variations of l_1 and l_2. Therefore, when the cutting height remains constant, the horizontal swing of the cutting mechanism can be controlled by regulating the extension and retraction amount l_2 of the rotary hydraulic cylinder. When the cutting mechanism swings in the opposite direction, it is only necessary to change l_1 to $-l_1$, l_2 to $-l_2$, and α to $-\alpha$ in the

expression.

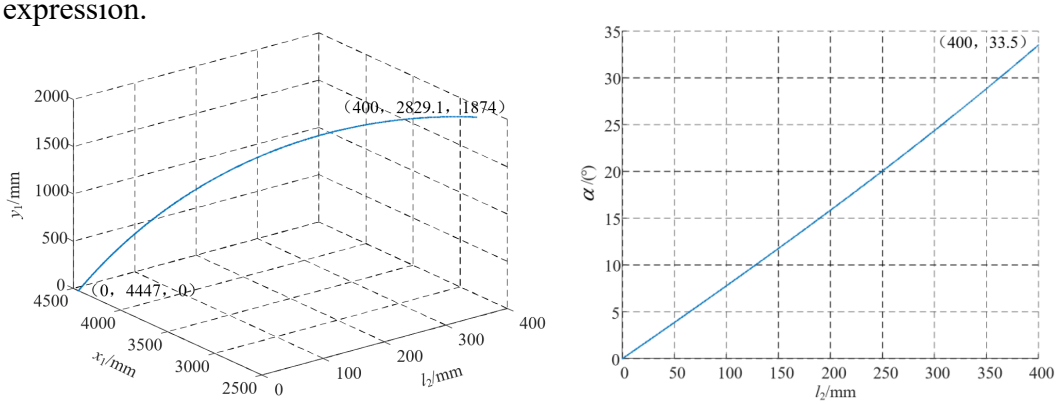

(a) The relationship between the cutting head position and l_2

(b) The relationship between the horizontal swing Angle and l_2

Fig. 4. Simulation of horizontal oscillating cutting of cutting mechanism

It can be seen from Fig. 4(a) that the position coordinate x_1 of the cutting head decreases in a parabolic pattern from 4447 mm to 2829.1 mm with the increase of l_2, while the coordinate y_1 rises in a straight line from 0 mm to 1874 mm. As can be seen from Fig. 4(b), the horizontal swing Angle α increases linearly with the increase of l_2, and the maximum swing Angle is 33.5° , which is basically consistent with the maximum swing Angle during the actual cutting process of the tunnel boring machine.

By conducting a comprehensive analysis of equations (1) to (4), the matrix expression of the spatial position (x_1, y_1, z) of the cutting head and the swing Angle of the cutting mechanism joint can be obtained:

$$\begin{bmatrix} x_1 \\ y_1 \\ z \end{bmatrix} = \begin{bmatrix} e\cos\alpha \\ e\sin\alpha \\ 0 \end{bmatrix} + \begin{bmatrix} (L_x+\Delta l)\cos\theta\cos\alpha \\ (L_x+\Delta l)\cos\theta\sin\alpha \\ (L_x+\Delta l)\sin\theta \end{bmatrix} = \begin{bmatrix} [e+(L_x+\Delta l)\cos\theta]\cos\alpha \\ [e+(L_x+\Delta l)\cos\theta]\sin\alpha \\ (L_x+\Delta l)\sin\theta \end{bmatrix} \quad (5)$$

According to Fig. 5(a), the minimum value of the cutting head coordinate x_1 is 2829.1mm, and the maximum value is 4447mm, and x_1 decreases parabolically with the increase of l_1 and l_2; From Fig. 5(b), it can be seen that the minimum value of the cutting head coordinate y_1 is 0 and the maximum value is 1874mm, and y_1 increases linearly with the increase of l_1 and l_2; From Fig. 5(c), it can be seen that the minimum value of the cutting head coordinate z is 0mm and the maximum value is 2604.9mm, and z increases linearly with the increase of l_1 and l_2; From Fig. 5(d), it can be seen that the trajectory of the cutting head follows a spatial parabolic motion pattern. When x_1 is at its maximum, y_1 and z are at their minimum, while when x_1 is at its minimum, y_1 and z reach their maximum values.

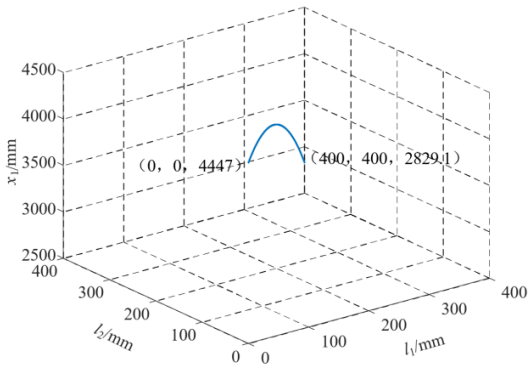

(a) The relationship curve between coordinate x_1 and l_1, l_2

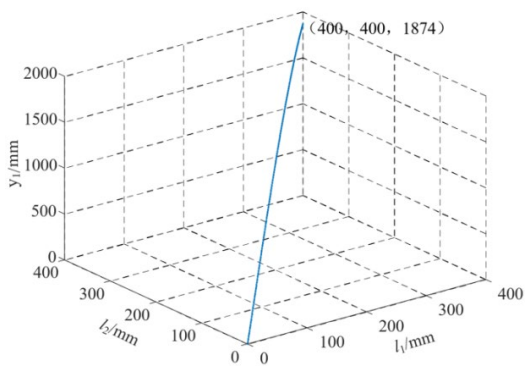

(b) The relationship curve between coordinate y_1 and l_1, l_2

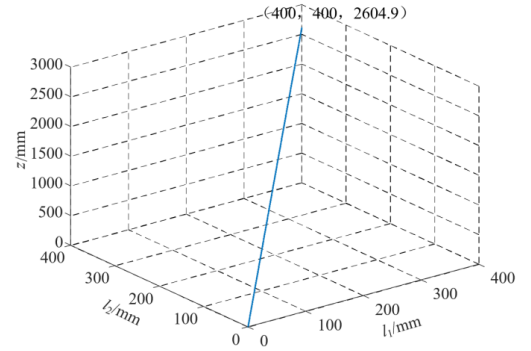

(c) The relationship curve between coordinate z and l_1, l_2

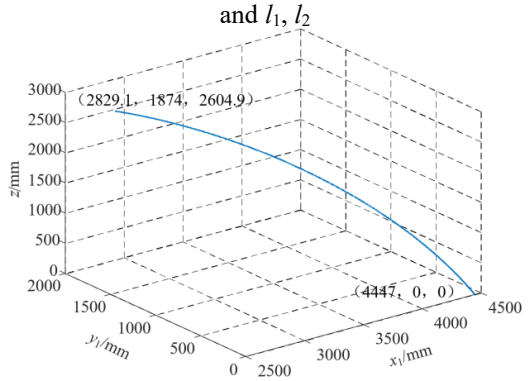

(d) The movement trajectory curve of the cutting head

Fig. 5. Simulation diagram of the spatial position coordinates of cutting head

By transforming the above formula, the kinematic relationship between the expected coordinates (y_1, z) of the cutting head and the displacements l_1 of the lifting hydraulic cylinder and l_2 of the rotating hydraulic cylinder is obtained, thereby determining the motion trajectory equation of the cutting head:

The motion trajectory equation of the cutting head is determined:

$$\begin{cases} l_1 = \sqrt{L_1^{\,2} + L_2^{\,2} - 2L_1L_2\cos\left(F(z,\ \Delta l) + \phi_0 - \theta_0\right)} - L_0 \\ l_2 = \sqrt{n^2 + R^2 - 2nR\cos\left(\theta_1 + F(y_1, z, \Delta l)\right)} - L_3 \end{cases} \tag{6}$$

In addition, the influence of the roadheader's vibration on the trajectory tracking control of the cutting head should be considered. Subsequently, by controlling the displacement of the lifting and slewing hydraulic cylinders according to Equation (6), the vertical and horizontal oscillation of the cutting head can be regulated, thereby achieving the tracking control of the cutting head's motion trajectory.

3. Control of the movement trajectory of the cutting head of the roadheader

3.1 Dynamic analysis of the cutting mechanism

1) Dynamic analysis of the rotary cutting mechanism

As shown in Fig. 6, during the horizontal swinging process of the roadheader to cut coal and rock, the main load of the rotary cutting mechanism comes from the cutting resistance F_x of the coal and rock on the cutting head.

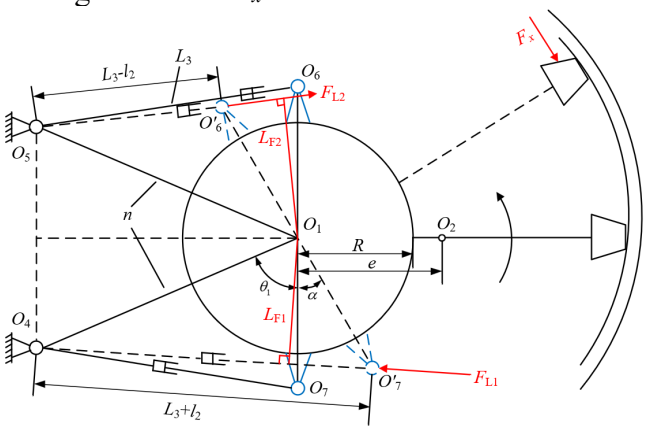

Fig. 6. Schematic diagram of force analysis of rotary cutting mechanism

Based on the analysis of the kinematics of the rotary cutting mechanism, the dynamic equation of the rotary cutting mechanism is established[13]:

$$J_1\frac{d^2\alpha}{dt^2}=\frac{nR\sin(\alpha+\theta_1)}{L_3+l_2}F_{L1}-M_{f1}-F_x(L_x\cos\theta+e)+\frac{nR\sin(\alpha-\theta_1)}{L_3-l_2}F_{L2} \quad (7)$$

In the formula: J_1 represents the moment of inertia of the back-cutting mechanism, kg.m^2; M_{f1} represents the rotational friction torque, in N.m; F_x is the cutting resistance of the cutting head, N; F_{L1} and F_{L2} are respectively the external load forces of the left and right rotary hydraulic cylinders, in N.m.

The rotary cutting mechanism operates slowly, and its frictional torque and inertial torque can be ignored[14]. The dynamic equation is simplified as:

$$F_x(L_x\cos\theta+e)=\frac{nR\sin(\alpha+\theta_1)}{L_3+l_2}F_{L1}+\frac{nR\sin(\alpha-\theta_1)}{L_3-l_2}F_{L2} \quad (8)$$

External loads on the piston rods of the left and right rotary hydraulic cylinders:

$$\begin{cases}F_{L1}=\dfrac{\pi}{4}D_a^2p_1-\dfrac{\pi}{4}(D_a^2-d_a^2)p_2\\ F_{L2}=\dfrac{\pi}{4}(D_a^2-d_a^2)p_1-\dfrac{\pi}{4}D_a^2p_2\end{cases} \quad (9)$$

In the formula: D_a is the internal diameter of the cylinder body, m; d_a is the diameter of the piston rod, m; p_1 is the inlet chamber pressure, MPa; p_2 is the pressure in the return oil chamber, MPa。

According to Equation (9), select d_a=0.6d_a to obtain the ratio of the system oil to the external load of the piston rods of the left and right rotating hydraulic cylinders, that is, F_{L1}:F_{L2}=1:0.64. According to Equation (8), by substituting the relevant parameters such as the cutting resistance F_x of the cutting head under the horizontal cutting condition, the mathematical relationship between the external load force (F_{L1}、 F_{L2}) of the hydraulic cylinder and the cutting resistance F_x can be determined.

2) Dynamic analysis of the lifting and cutting mechanism

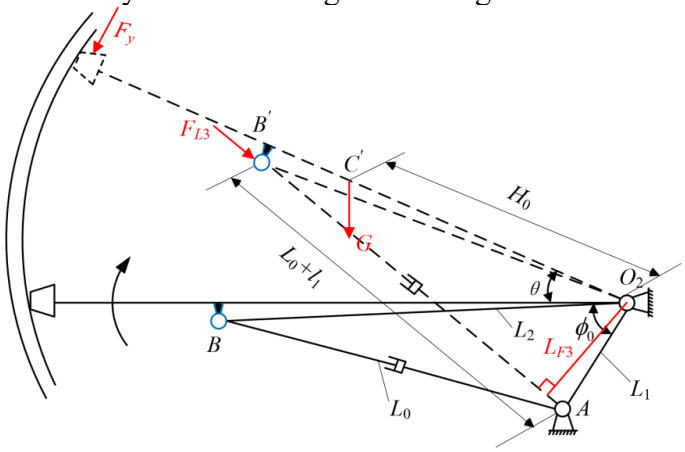

Fig. 7. Schematic diagram of force analysis of lifting and cutting mechanism

As shown in Fig. 7, during the vertical swinging process of the roadheader to cut coal and rock, the main load of the lifting and lowering cutting mechanism comes from the radial resistance F_y of the coal and rock on the cutting head and the weight G of the cantilever itself.

Based on the analysis of the kinematics of the lifting cutting mechanism, the dynamic equation of the lifting cutting mechanism is established[15,16]**:**

$$J_2 \frac{d^2\theta}{dt^2} = 2\frac{L_1 L_2 \sin(\phi_0+\theta)}{L_0+l_1} F_{L3} - GH_0\cos\theta - L_x F_y - M_{f2} \tag{10}$$

Similarly, ignoring the frictional torque and inertial torque of the lifting and cutting mechanism, the dynamic equation is simplified as[16]:

$$L_x F_y = 2\frac{L_1 L_2 \sin(\phi_0+\theta)}{(L_0+l_1)} F_{L3} - GH_0\cos\theta \tag{11}$$

In the formula: J_2 represents the moment of inertia of the lifting and cutting mechanism, kg.m^2. G is the gravitational force of the cutting arm, N; H_0 is the distance from the vertical swing center O_2 of the cutting arm to the center of

gravity of the cutting arm, m; F_y is the radial resistance of the cutting head, N; F_{L3} represents the external load force of the lifting hydraulic cylinder, N; M_{f2} represents the lifting friction torque, in N.m.

According to Equation (11), by substituting relevant parameters such as the radial resistance F_y of the cutting head under the vertical cutting condition, the mathematical relationship between the external load force F_{L3} of the hydraulic cylinder and the radial resistance F_y of the cutting head can be determined.

3.2 Control method for the movement trajectory of the cutting head

Based on the analysis of the inverse kinematics and dynamics of the cutting mechanism, a cutting head motion trajectory tracking control method is proposed, as shown in Fig. 8.

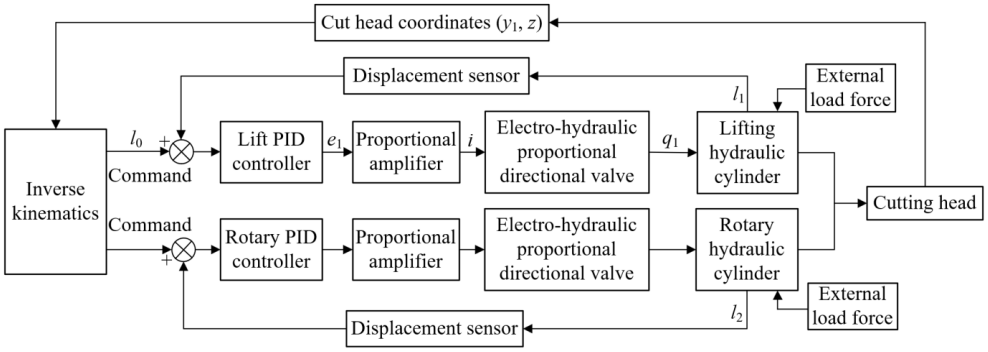

Fig. 8. Cutting head trajectory tracking control method

In Fig. 8, l_0 represents the target displacement of the hydraulic cylinder, in mm; e_1 is the input voltage of the proportional amplifier, V; i is the output current of the proportional amplifier, A; q_1 represents the load flow rate, m^3/s.

According to the research results at home and abroad, the vibration mode of the cutting head is multi-degree-of-freedom periodic forced vibration; Therefore, it can be assumed that the vibration mode of the cutting head is a sine wave. According to the cutting conditions of the tunnel boring machine, the vibration functions $f_x(t)=A\sin wt$ and $f_y(t)=B\sin wt$ of the cutting head are constructed respectively in the horizontal and vertical directions. In addition, the load on the cutting head, as an external excitation, to a certain extent determines the vibration degree of the cutting head. Therefore, the mathematical relationship between the cutting resistance F_x, the radial resistance F_y and the vibration function of the cutting head can be established, this paper will not elaborate further.

The input and output impedances of a proportional amplifier differ significantly. The transfer function after the proportional link is regarded as[16]:

$$\frac{I(s)}{E_1(s)} = K_v \tag{12}$$

In the formula, $I(s)$, $E_1(s)$, and K_v represent the output current (in A), input

voltage (in V), and gain of the proportional amplifier, respectively.

The electro-hydraulic proportional directional control valve link can be approximately regarded as a second-order control link in practical engineering applications[16,17], and its transfer function is:

$$\frac{Q_1(s)}{I(s)} = \frac{K_t}{\frac{s^2}{W_v^2} + \frac{2\delta_v}{W_v}s + 1} \tag{13}$$

In the formula, K_t, W_v, and δ_v represent the flow gain (in m^3/s.A), phase bandwidth (in rad/s), and damping ratio (ranging from 0.5 to 0.7) of the electro-hydraulic proportional directional valve, respectively.

The hydraulic cylinder studied in this paper is an asymmetric hydraulic cylinder controlled by an electro-hydraulic proportional directional control valve. By performing Laplace transformation on the flow equation of the valve, the flow equation of the hydraulic cylinder, and the load force balance equation, the transfer function of this link is determined[16]:

$$\frac{L}{Q_1} = \frac{1/A_h}{s\left(\frac{s^2}{W_b^2} + \frac{2\delta_b}{W_b}s + 1\right)} \tag{14}$$

In the formula, A_h, W_b, and δ_b represent the rodless cavity area (in m^2), natural frequency (rad/s), and damping ratio (ranging from 0.1 to 0.2) of the hydraulic cylinder, respectively.

Since the bandwidth of the position detector is higher than that of the system, it can be approximately regarded as a proportional link, and its transfer function is[16,18]:

$$\frac{Y(s)}{L(s)} = K_w \tag{15}$$

In the formula: K_w represents the gain of the position detection sensor.

Based on the motion trajectory tracking control method of the cutting head, the transfer functions of each link in the control system without load are determined by equations (12) to (15), and the input of the load link is determined according to the mathematical relationship between the vibration function of the cutting head and the external load force of the hydraulic cylinder. Thus, the transfer function model of the tunnel boring machine control system is established, as shown in Fig. 9. When conducting vertical swing cutting or horizontal swing cutting simulations of the cutting head, it is only necessary to substitute the corresponding simulation parameters into the transfer function model of the control system.

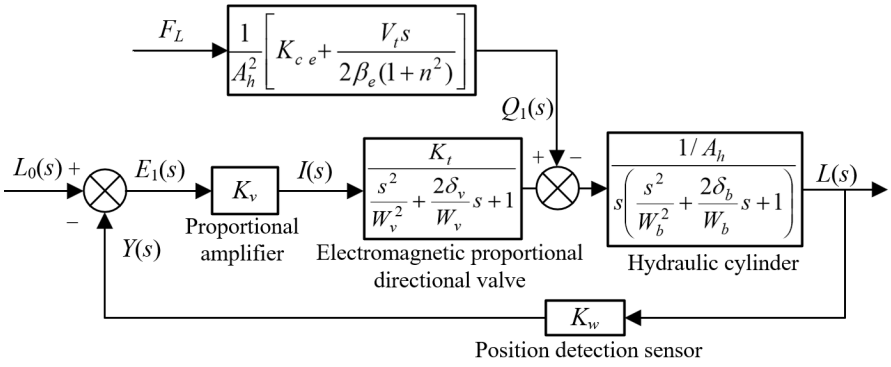

Fig. 9. Transfer function model of boom-type roadheader control system

In Fig. 9, $L_0(s)$, $E_1(s)$, $I(s)$, $Q_1(s)$, and $L(s)$ are respectively the expressions when calculating the transfer functions l_0, e_1, i, q_1, and $l(l_1$、$l_2)$ as shown in Fig. 8.

Then the open-loop transfer function of this control system is[16,19]:

$$L(s)=\frac{L_0(s)K_vK_t/A_h\left(\frac{s^2}{W_b^2}+\frac{2\delta_b}{W_b}s+1\right)-\frac{1}{A_h^3}\left[K_{ce}+\frac{V_t s}{2\beta_e(1+n^2)}\right]F_L}{s\left(\frac{s^2}{W_v^2}+\frac{2\delta_v}{W_v}s+1\right)}\bullet K_w \quad (16)$$

When the roadheader is not under load, that is, when the roadheader does not cut through the coal or rock, the open-loop amplification factor of the control system is approximately[16]:

$$K_n=K_vK_tK_w/A_h \quad (17)$$

3.3 Simulation of the motion trajectory control system for the cutting head

Taking the EBZ200 roadheader as an example, some parameters of the roadheader were determined[16,20], as shown in Table 2.

Table 2

Part parameters of EBZ200 roadheader

Parameter name	Numerical value	Parameter name	Numerical value
Inner diameter of the rotary cylinder	160mm	Inner diameter of the lifting cylinder	180mm
Outer diameter of the rotary cylinder	194mm	Outer diameter of the lifting cylinder	219mm
Range of the horizontal swing Angle	-32°~32°	Vertical swing Angle range	-31°~42°
Rod diameter of the rotary oil cylinder	100mm	Rod diameter of lifting cylinder	110mm
Rotary table quality	2250Kg	Cutting arm quality	9363Kg

Rotary cylinder stroke	870mm	Lift cylinder stroke	620mm
Expansion and contraction of cutting head	650mm	Cut off arm length	3747mm
Mass of a single rotary hydraulic cylinder	219Kg	Quality of a single lifting hydraulic cylinder	234Kg
Total volume of two chambers of rotary hydraulic cylinder	28L	Total volume of the two chambers of the lifting hydraulic cylinder	27L

Based on the transfer function model of the tunnel boring machine control system, the simulation parameters of the cutting head motion trajectory control system under different cutting conditions were calculated using the parameter values in Table 2, as shown in Table 3.

Table 3

Simulation parameters of the cutting head trajectory control system

The cutting head moves horizontally	K_v=0.031	K_t=2.5×10^{-3} m^3/s.A	δ_v=0.7	W_v=157.1rad/s
	A_h=2.01×10^{-2} m^2	δ_b=0.2	W_b=33rad/s	K_w=7.36V/m
The cutting head moves vertically	K_v=0.031	K_t=2.48×10^{-3} m^3/s.A	δ_v=0.7	W_v=157.1rad/s
	A_h=2.54×10^{-2} m^2	δ_b=0.2	W_b=42rad/s	K_w=11.77V/m

Based on the transfer function model of the tunnel boring machine control system, the simulation models of the control system for the horizontal and vertical movement directions of the cutting head were established in the Simulink module, as shown in Fig. 10. To ensure the safety of tunnel construction, the cutting head of the tunnel boring machine is not allowed to extend during the cross-sectional cutting process. Therefore, when simulating the control system, the extension and retraction amount Δl of the cutting head is set to 0.

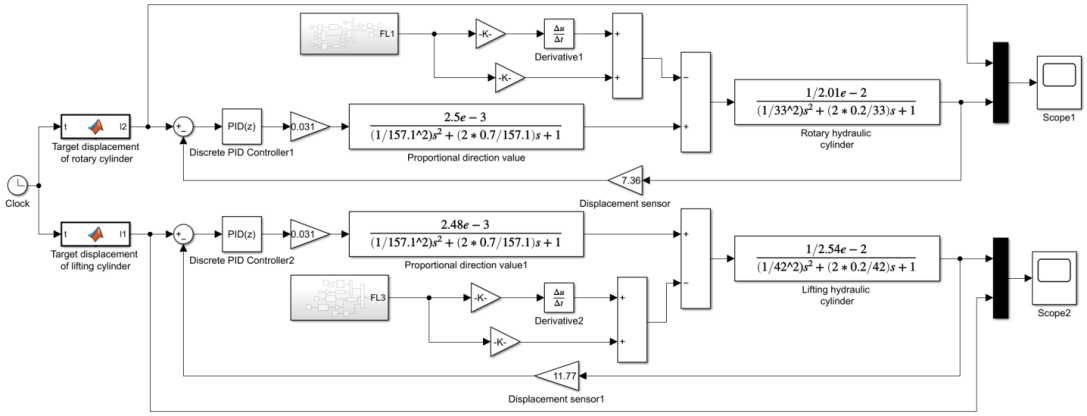

Fig. 10. Cutting head trajectory control system simulation model

Given the parameter equation of the cutting head spatial motion trajectory, based on the simulation model of the cutting head motion trajectory control system, the cutting head trajectory is tracked and controlled through simulation。

$$\begin{cases} y_1 = 0.003 \cdot t \\ z = 1.404 + 0.3\sin(0.03\pi \cdot t) \end{cases} \tag{18}$$

Input the established motion trajectory equation of the cutting head into the MATLAB/Function module to generate the target displacements of the rotary and lifting hydraulic cylinders, and set the system simulation time to 60 seconds.

As shown in Fig. 11, the displacement of the piston rod of the lifting hydraulic cylinder reaches its maximum value at 16.67 s, which is 66.25 mm. The minimum value was achieved at the 50 s, which was -64.82 mm. Affected by the vibration characteristics of the cutting head, the simulation displacement curve of the piston rod of the lifting hydraulic cylinder fluctuates throughout the entire process, but it is basically consistent with the target displacement curve.

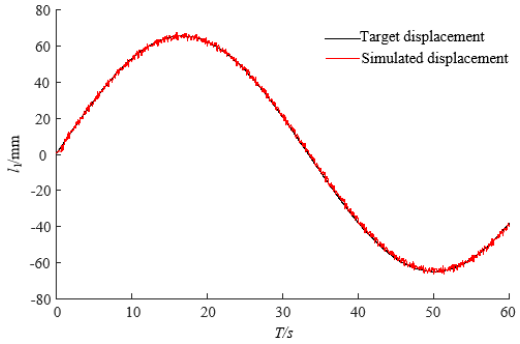

Fig 11. Lift hydraulic cylinder displacement curve

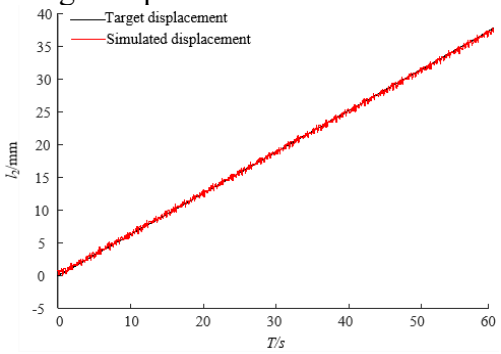

Fig 12. Displacement curve of rotary hydraulic cylinder

As shown in Fig. 12, within 0 to 60 s, the piston rod of the rotary hydraulic cylinder extended by 37.78 mm. Affected by the vibration characteristics of the cutting head, the simulation displacement curve of the piston rod of the rotary hydraulic cylinder fluctuates throughout the entire process, but it is basically consistent with the target displacement curve.

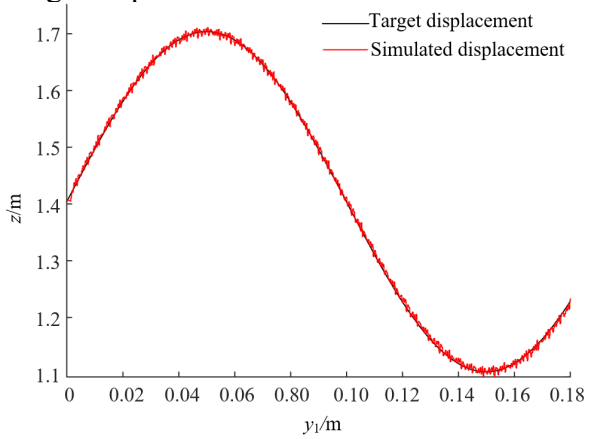

Fig. 13. Cutting head motion trajectory tracking control curve

As shown in Fig. 13, the trajectory tracking error when the cutting head moves vertically is controlled within 5.2 mm, and the trajectory tracking error when the cutting head moves horizontally is controlled within 4.3 mm. Affected

by the vibration characteristics of the cutting head, the simulation trajectory of the cutting head changes in a fluctuating pattern throughout the entire process, but it is basically consistent with the target trajectory of the roadway section, which proves the correctness of the trajectory tracking control method of the cutting head.

4. Conclusions

In order to achieve the tracking and control of the motion trajectory of the cutting head under vibration interference and improve the forming quality of the roadway section, the kinematics inverse solution simulation of the cutting mechanism was carried out in this paper through MATLAB software, and the model simulation of the motion trajectory control system of the cutting head was conducted in the Simulink module. The conclusions are as follows：

1) The vertical and horizontal swing kinematic models of the cutting mechanism were established, and the inverse kinematics simulation of the cutting mechanism was carried out. The motion trajectory equation of the cutting head was obtained, which will be used for the subsequent research on the trajectory planning and tracking control of the cutting head.

2) A cutting head motion trajectory tracking control method was proposed, and a cutting head motion trajectory control system was established through MATLAB/Simulink. Simulation analysis was conducted, and the simulated trajectory was basically consistent with the target trajectory. Compared with the simulation results in reference [21,22], the correctness of the proposed cutting head motion trajectory tracking control method was verified.

3) A cutting head motion trajectory tracking control method under vibration interference was proposed. A cutting head motion trajectory control system was established using MATLAB/Simulink, and simulation analysis was conducted. The simulated trajectory obtained was basically consistent with the target trajectory, verifying the correctness of the proposed cutting head motion trajectory tracking control method.

This article adopts a combination of theory and simulation to obtain the above conclusions, but the proposed cutting head motion trajectory tracking control method only conducts simulation analysis. If combined with experimental verification, the research conclusions will have more guiding significance.

REFERENCES

[1] *Zeki*. Evaluation of current TBM cutting head design and recommendations for improving machine performance. International Journal of Mining, Reclamation and Environment, 2024, 38(3): 193-213.

[2] *Xie*. Research on the Application of Automatic Cutting System for Tunnel Boring Machine. Mechanical Management and Development, 2023(12): 182-184.
[3] *Peng, Chu, He*, et al. Joint Simulation Study on Cutting Track Control of Cantilever Tunneling Machine. Machine Tool and Hydraulic, 2023, 51(08): 130-136.
[4] *Zhang, Chen, Ding*, et al. Research on Virtual and Real Fusion Experiment System of Cutting Part of Cantilever Tunneling Machine. PloS one, 2025, 20(8): e0330291
[5] *Zhang, Zhang, Yang*, et al. A Planning Method for Cutting Path of Cantilever Tunneling Machine Based on Improved NSGA-II. Applied Sciences, 2025, 15 (4): 2126-2126.
[6] *Liu*. Research on Automatic Control Technology of Cutting Head Speed and Torque of Excavator. Coal Mining Machinery, 2025(02): 50-53.
[7] *Liang, Tian, Huo*. Finite Element Simulation Study on Cutting Coal and Rock by Cutting Head of Tunnel Boring Machine. Journal of Physics: Conference Series, 20232591 (1).
[8] *Ma, Zhang, Yang*, et al. Research on positioning accuracy of cutting head of roadheader based on ultra-wide band positioning technology. Process, 2023, 11(9).
[9] *Qin*. Research on Automatic Cutting Technology of Cantilever Tunneling Machine. Coal Mine Machinery, 2023(12): 52-55.
[10] *Xie, Shi, Zhang*, et al. Prediction of Longitudinal Vibration Characteristics of New Longitudinal Shaft Tunneling Machine under Multi-excitation. Journal of Engineering Design, 2023(6): 728-737.
[11] *Tan, Tan, Ye*, et al. Kinematic Study on Cutting Mechanism of Longitudinal Shaft Tunneling Machine. Mining Machinery, 2014, (12): 31-36.
[12] *Kang, Liu, Ma*, et al. Transient dynamic analysis of cutter-head loads: effects of different cutter spacings during excavation. Frontiers in Earth Science, 2025, 12.
[13] *Chantal, Lu, Liu*, et al. Analysis of dual-driven feed system vibration characteristics based on computer numerical control machine tools: a systematic review. Symmetry, 2023, 15(11): 2012.
[14] *Cheluszka, Mann*. Vibration identification of the roadheader cutting head using high-speed cameras. MATEC Web of Conferences, 2019, 252: 3018.
[15] *Hekimoglu*. Investigations into tilt angles and order of cutting sequences for cutting head design of roadheaders. Tunnelling and Underground Space Technology, 2018, 76: 160-171.
[16] *He*. Simulation study on automatic cutting control of cantilever tunneling machine. Anhui University of Science and Technology, 2022.
[17] *Heyduk, Joostberens*. Automatic control of roadheader cutting head speed and load torque. IOP conference series. Earth and environmental science, 2020, 609(1): 12081.
[18] *Chaudhary, Prasad, Prasad*, et al. Robot motion control using stepping ahead firefly algorithm and kinematic equations. IEEE Access, 2024, 12: 43078-43088.
[19] *Tian, Wang, Wu*. Dynamic Characteristic Analysis of Tunneling Automatic Cutting and Forming Control System. Industrial and Mining Automation, 2015 (6): 40-44.
[20] *Wang, Gao, Li*, et al. Automatic cutting and forming control system for arbitrary roadway section based on PCC. Journal of Coal Industry, 2013(S1): 261-266.
[21] *Bhoyar, Kumar*. Review on design and analysis of drill head of boring machine by using vibration conditioning monitoring. International journal for research in applied science and engineering technology, 2023, 11(5): 1379-1382.
[22] *Mao*, *Chen*, *Yan*, et al. Accurate control method for cutting head position of cantilever tunneling machine in coal mines. Journal of Coal Industry, 2017, 42 (S2): 562-567.